

Reconstructing simplicial complexes from evolutionary games

Yin-Jie Ma,^{1,2,3} Zhi-Qiang Jiang,^{1,2,*} Fanshu Fang,^{3,4} Charo I. del Genio,^{5,6,†} and Stefano Boccaletti^{3,6,7}

¹*School of Business, East China University of Science and Technology, Shanghai, China*

²*Research Center for Econophysics, East China University of Science and Technology, Shanghai, China*

³*CNR - Institute of Complex Systems, Via Madonna del Piano 10, I-50019, Sesto Fiorentino, Italy*

⁴*College of Economics and Management, Nanjing University of Aeronautics and Astronautics, Nanjing, China*

⁵*Institute of Smart Agriculture for Safe and Functional Foods and Supplements, Trakia University, Stara Zagora 6000, Bulgaria*

⁶*Research Institute of Interdisciplinary Intelligent Science,
Ningbo University of Technology, 315104, Ningbo, China*

⁷*Sino-Europe Complexity Science Center, School of Mathematics,
North University of China, 030051, Taiyuan, China*

(Dated: March 21, 2025)

In distributed systems, knowledge of the network structure of the connections among the unitary components is often a requirement for an accurate prediction of the emerging collective dynamics. However, in many real-world situations, one has, at best, access to partial connectivity data, and therefore the entire graph structure needs to be reconstructed from a limited number of observations of the dynamical processes that take place on it. While existing studies predominantly focused on reconstructing traditional pairwise networks, higher-order interactions remain largely unexplored. Here, we introduce three methods to reconstruct a simplicial complex structure of connection from observations of evolutionary games that take place on it, and demonstrate their high accuracy and excellent overall performance in synthetic and empirical complexes. The methods have different requirements and different complexity, thereby constituting a series of approaches from which one can pick the most appropriate one given the specific circumstances of the application under study.

I. INTRODUCTION

Complex networks provide a powerful framework to study a broad range of systems [1–3]. Traditional networks consist of a number of links, called edges, between pairs of discrete elements, called nodes. Their use has proved highly successful in numerous applications, which include determining the functional modules of the human brain [4], describing the dynamics of gene expression [5], detecting the presence of communities in large data sets [6–8], modelling the emergence of strategy in social interactions [9–13], and suggesting the formulation of new antimicrobials [14, 15]. Moreover, they have been a fundamental tool in investigating the properties of dynamical processes such as epidemic and information spreading [16–18], evolutionary games [19], and synchronization of coupled oscillators [20–22]. However, a limitation of the original network paradigm has recently come to light, with the realization that many complex systems feature multi-body interactions, whereby macroscopic effects result from collective contributions, each involving three or more nodes [23].

Accounting for the presence of higher-order interactions induces a profound change in the mathematical structure of the networks. In fact, while traditional networks are usually described by simple graphs, higher-order networks are best represented as hypergraphs, which are collections of edges that can link any number of nodes. A special case occurs when the presence

of a collective interaction between the members of a set of nodes induces additional interactions amongst all possible smaller subsets of the same nodes. The resulting structure is then a particular case of a hypergraph, which takes the name of *simplicial complex*. Numerous theoretical advances in the study of hypergraphs and simplicial complexes have been accomplished over the last decade. However, virtually all network methods rely on the knowledge of the global structure, which is often not accessible when investigating real-world systems. Thus, researchers are forced to find ways to infer or reconstruct the unknown links from limited observations.

Because of this, the inverse problem of determining the structure of a network from partial data has sparked a notable amount of interest, and many methods to achieve this goal have been developed. Depending on the nature of the approach they take, these can be roughly ascribed to two types, namely the statistical ones [24–28], which aim to detect the edges in the network using inference methods, and the optimization ones [29–33], which turn the global task into a set of sub-problems of convex optimization with linear constraints. Within this latter class, compressive sensing has gained a great popularity during the last decade [34]. The main idea behind the technique is to take a series of observations, whose nature depends on the specific kind of system being reconstructed, and use it to derive a set of underdetermined linear equations. In the assumption that the network is sparse, which is almost always true in real-world situations [35], one can then solve the system and produce local estimates of the adjacency matrix, which encodes the full connectivity of the network. Note that, despite the effectiveness of compressive sensing, care must be taken to ensure that the re-

* Corresponding author: zqjiang@ecust.edu.cn

† Corresponding author: charo.delgenio@trakia-uni.bg

Payoffs in pairwise games			
		s_j	
		C	D
s_i	C	1, 1	S, T
	D	T, S	0, 0

Payoffs in three-body games					
		s_j (when $s_k = C$)		s_j (when $s_k = D$)	
		C	D	C	D
s_i	C	1, 1, 1	G, T, G	G, G, T	S, W, W
	D	T, G, G	W, W, S	W, S, W	0, 0, 0

Figure 1. **Payoff matrices for evolutionary games.** If the players’ strategy s is to cooperate (C) or defect (D) all at the same time, they all receive a unitary reward or nothing, respectively. If a player is the only one to cooperate or defect, it receives a sucker’s payoff S or a temptation payoff T . In three-body games, two players who cooperate against a single defector receive a payoff G , whereas two players who defect against a single cooperator receive a payoff W .

sults obtained are consistent. For example, in undirected networks, one must ensure that the resulting adjacency matrix is symmetric, which can be achieved via the inclusion of latent constraints [31]. It is also worth noticing that such constraints may go beyond the symmetry ones when higher-order interactions are considered [36], and their number grows quickly with the order of the edges. Thus, developing an efficient reconstruction method for higher-order networks is a serious challenge.

In this article, we propose a novel framework for reconstructing simplicial complexes that effectively captures higher-order interactions in dynamic real-world settings, where equilibrium is often impractical due to the fluctuating nature of social and strategic interactions. A key distinction of our approach is the utilization of transient-phase data from evolutionary games, rather than relying on equilibrium states or non-equilibrium steady states. Unlike the latter, transient phases provide richer dynamical information, encoding the system’s pathway toward equilibrium and offering a more effective means of inferring higher-order structures. Transient dynamics frequently emerge in evolutionary games, such as coordination games on complex networks [37], prisoner’s dilemma with adaptive strategies [38], and public goods games with reputation-driven interactions [39], which reinforce the relevance of our approach. Our framework is based on compressive sensing techniques and includes a point-by-point estimator (PBP), a global estimator (GLO), and a global estimator with simplicial constraints (GLOC). Furthermore, we demonstrate the robustness of our methods by evaluating their performance under noisy conditions, showing that GLOC achieves relatively higher accuracy, even with smaller observation data sets. By capturing the evolving nature of interactions, our framework provides a systematic and practical approach to reconstructing higher-order structures from dynamic real-world data.

The remainder of the article is organized as follows: in Section II, we describe the formalism of evolutionary games we adopt; in Section III we rigorously formulate the reconstruction problem and discuss PBP, GLO and GLOC in detail; in Section IV we briefly introduce

the different methods we use to create synthetic complexes, or to construct complexes from empirical data, as well as the metrics we use to assess the performance of our methods; in Section V we present the results of the three methods on synthetic complexes and on empirical ones; finally, we give our concluding remarks in Section VI.

II. FORMALISM OF EVOLUTIONARY GAMES

Evolutionary dynamics is often used as a paradigmatic model to study the formation of complex social interactions between agents on a network. In general, the dynamics of an evolutionary game advances via two steps, namely computing the payoffs that players receive according to the combination of their choices, and updating each player’s strategy according to the state of the system at any given moment in time.

Here, we consider four classic games, namely the Prisoner’s Dilemma, the Stag Hunt, the Snowdrift and the Harmony game. To reduce the computational costs, and focus on the effectiveness of our methods, we only consider pairwise and three-body interactions. However, our approaches can be straightforwardly generalized to edges of any size. Also note that, conventionally, an edge linking d nodes is called a $d - 1$ -simplex. Thus, simple edges, corresponding to pairwise interactions, are 1-simplices, whereas edges representing triadic interactions are 2-simplices. All four games we use represent situations in which players choose between cooperative behaviour (C) and individualistic defection (D). Thus, when a game is being played by 2 players at a time, i.e., on a 1-simplex, there are 4 possible cases, whereas the total number of possible outcomes is 8 when the game is played by 3 players at a time, i.e., on a 2-simplex. As illustrated schematically in Fig. 1, in pairwise games both players receive a unitary reward when they cooperate with each other, and receive nothing if they both defect. If one player cooperates while the other defects, then the cooperating one receives a so-called sucker’s payoff S , and the defecting one receives the temptation pay-

off T . In three-body games, the players still receive a unitary reward or nothing for cooperating or defecting all together, respectively, and a player's payoff is still S or T when they are the only one to cooperate or defect, respectively. However, in these last two cases, the other two players receive a payoff W for defecting or a payoff G for cooperating.

Note that the difference in the equilibrium states of the four games is determined by the values of T and S . Specifically, in the Prisoner's Dilemma, for which $T > 1$ and $S < 0$, the only Nash equilibrium is mutual defection. In the Harmony game, which has the opposite relations $T < 1$ and $S > 0$, mutual cooperation prevails. In the Snowdrift game, where $T > 1$ and $S > 0$, the equilibrium states feature one player cooperating and the other one defecting. Finally, in the Stag Hunt, with $T < 1$ and $S < 0$, the equilibrium states have both players either cooperating or defecting at the same time. The Nash equilibria for three-body games, however, are more complex, and depend on the deviation between W and G [40].

In a simplicial complex of N players, denoting the strategy of player i at round t_m as $s_i(t_m)$, the total payoff for player i at that round, $\pi_i(t_m)$, is obtained by summing the individual contributions from each simplex it participates in:

$$\begin{aligned} \pi_i(t_m) = & \sum_{j=1}^N A_{i,j}^{(1)} P_{i,j}^{(1)}(t_m) \\ & + \sum_{\substack{j_1, j_2=1 \\ j_1 < j_2}}^N A_{i,j_1,j_2}^{(2)} P_{i,j_1,j_2}^{(2)}(t_m). \end{aligned} \quad (1)$$

In the equation above, $\mathbf{A}^{(1)}$ and $\mathbf{A}^{(2)}$ are the adjacency matrix of the 1-simplices and the adjacency tensor of the 2-simplices, respectively, and their elements are 1 if an edge exists on the nodes corresponding to their indices, and 0 otherwise. Also, $\mathbf{P}^{(1)}(t_m)$ and $\mathbf{P}^{(2)}(t_m)$ are the payoff matrix and the payoff tensor for pairwise and three-body interactions at time t_m , respectively, and their (i, j) or (i, j_1, j_2) elements are the reward that player i receives if it participates in a game with player j or with players j_1 and j_2 , given a choice of strategies.

At each time step, players update their strategies based on a simple imitation rule: random selection among neighbors. Specifically, at the beginning of each round, each player randomly selects one of their neighbors and adopts their last strategy for the next turn. This rule ensures that strategies do not rapidly converge to equilibrium, allowing us to capture richer transient-phase dynamics over a longer observation period [30]. In real-

world social systems, where equilibrium is often impractical due to the dynamic and fluctuating nature of interactions, relying on transient-phase data provides a more realistic representation of higher-order structures.

III. SIMPLICIAL COMPLEX RECONSTRUCTION

A. Problem formulation

The goal of our higher-order network reconstruction methods is to determine the structure of unknown simplicial complexes from observations of the payoffs and of the strategies of the nodes at M different times. In other words, we aim to find $\mathbf{A}^{(1)}$ and $\mathbf{A}^{(2)}$ from the payoff matrix $\mathbf{\Pi}$ and the strategy matrix \mathbf{S} , whose columns contain the time series of payoffs and strategies for the corresponding players, and have the form

$$\mathbf{\Pi} = \begin{pmatrix} \pi_1(t_1) & \pi_2(t_1) & \cdots & \pi_N(t_1) \\ \pi_1(t_2) & \pi_2(t_2) & \cdots & \pi_N(t_2) \\ \vdots & \vdots & \ddots & \vdots \\ \pi_1(t_M) & \pi_2(t_M) & \cdots & \pi_N(t_M) \end{pmatrix}, \quad (2)$$

and

$$\mathbf{S} = \begin{pmatrix} s_1(t_1) & s_2(t_1) & \cdots & s_N(t_1) \\ s_1(t_2) & s_2(t_2) & \cdots & s_N(t_2) \\ \vdots & \vdots & \ddots & \vdots \\ s_1(t_M) & s_2(t_M) & \cdots & s_N(t_M) \end{pmatrix}. \quad (3)$$

The first step in reaching this goal is to note that, given M observations, all the equations concerning player i can be rewritten collectively as a system of linear equations. To do so, we introduce some auxiliary quantities. First, we call Π_i and $\hat{\Pi}_{t_m}$ the i -th column and the t_m -th row of $\mathbf{\Pi}$, respectively:

$$\Pi_i = (\pi_i(t_1), \pi_i(t_2), \dots, \pi_i(t_M))^T, \quad (4)$$

$$\hat{\Pi}_{t_m} = (\pi_1(t_m), \pi_2(t_m), \dots, \pi_N(t_m)). \quad (5)$$

Then, we build the matrices of time series of pairwise and three-body payoffs for player i ,

$$\Phi_i^{(1)} = \begin{pmatrix} P_{i,1}^{(1)}(t_1) & P_{i,2}^{(1)}(t_1) & \cdots & P_{i,N}^{(1)}(t_1) \\ P_{i,1}^{(1)}(t_2) & P_{i,2}^{(1)}(t_2) & \cdots & P_{i,N}^{(1)}(t_2) \\ \vdots & \vdots & \ddots & \vdots \\ P_{i,1}^{(1)}(t_M) & P_{i,2}^{(1)}(t_M) & \cdots & P_{i,N}^{(1)}(t_M) \end{pmatrix} \quad (6)$$

and

$$\Phi_i^{(2)} = \begin{pmatrix} P_{i,1,1}^{(2)}(t_1) & P_{i,1,2}^{(2)}(t_1) & \cdots & P_{i,1,N}^{(2)}(t_1) & P_{i,2,1}^{(2)}(t_1) & \cdots & P_{i,N,N}^{(2)}(t_1) \\ P_{i,1,1}^{(2)}(t_2) & P_{i,1,2}^{(2)}(t_2) & \cdots & P_{i,1,N}^{(2)}(t_2) & P_{i,2,1}^{(2)}(t_2) & \cdots & P_{i,N,N}^{(2)}(t_2) \\ \vdots & \vdots & \ddots & \vdots & \vdots & \ddots & \vdots \\ P_{i,1,1}^{(2)}(t_M) & P_{i,1,2}^{(2)}(t_M) & \cdots & P_{i,1,N}^{(2)}(t_M) & P_{i,2,1}^{(2)}(t_M) & \cdots & P_{i,N,N}^{(2)}(t_M) \end{pmatrix}. \quad (7)$$

Last, we build the adjacency flattenings for player i :

$$a_i^{(1)} = \left(A_{i,1}^{(1)}, A_{i,2}^{(1)}, \dots, A_{i,N}^{(1)} \right)^T \quad (8)$$

and

$$a_i^{(2)} = \left(A_{i,1,1}^{(2)}, A_{i,1,2}^{(2)}, \dots, A_{i,1,N}^{(2)}, A_{i,2,1}^{(2)}, \dots, A_{i,N,N}^{(2)} \right)^T. \quad (9)$$

Then, introducing the notations $\Phi_i = \left(\Phi_i^{(1)}, \Phi_i^{(2)} \right)$ and $A_i = \left(\left(a_i^{(1)} \right)^T, \left(a_i^{(2)} \right)^T \right)^T$, we can write

$$\Pi_i = \Phi_i \cdot A_i. \quad (10)$$

Note that, even though the strategies do not feature explicitly in the equation above, the elements of Φ_i and those of Π_i do depend on the choices of all the players that are connected to player i . Thus, the strategy matrix is implicitly entangled with the payoff one.

With this setup, solving the system in Eq. 10 for A_i allows one to reconstruct all the 1-simplices and 2-simplices in which player i participates, and the entire topology of the network can be estimated by repeating the procedure for every player. Then, a fundamental requirement is to ensure that the results obtained from the iterations of the procedure are consistent amongst themselves and with the nature of the network being reconstructed. To accomplish this, we propose three methods. First, we build a point-by-point estimator (PBP) to locally infer A_i ; then, we extend it to a global estimator (GLO); finally, we add simplicial constraints (GLOC), increasing the reconstruction accuracy for noisy data.

B. Point-by-point estimator

In the context of network reconstruction, the point-by-point (PBP) estimator is a local approach that infers the structure of a network by independently solving linear equations for each node [29, 41–43], based on observed dynamical data [44, 45]. This method involves estimating the connections of each node separately [46–48], without considering the global structure of the network [33, 49]. Specifically, assuming that the unknown network is sparse, a solution to Eq. 10 is given by

$$\arg \min_{\{A_i\} \mid \Pi_i = \Phi_i \cdot A_i} (\|A_i\|_1), \quad (11)$$

where $\|A_i\|_1$ is the 1-norm of A_i , i.e., the sum of its absolute values. Reconstruction of the whole network results

then from the union of the edges detected by solving the system for each individual node. Thus, this method is a point-by-point estimator (PBP) that builds a network from the local neighbourhoods of all the nodes. To mitigate the effect of noise on the measurements of Π_i , we include a 2-norm penalty in the equation above [33], so that the solution we seek is

$$\arg \min_{\{A_i\} \mid \Pi_i = \Phi_i \cdot A_i} (\|A_i\|_1 + \|\Pi_i - \Phi_i \cdot A_i\|_2). \quad (12)$$

Note that in this last equation the 1-norm is a structural quantity, as the elements of A_i constitute the local topology of the network, whereas the 2-norm is a temporal one, because the elements of Π_i relate to measurements at different moments.

We solve the last equation by applying the Orthogonal Matching Pursuit method [31]. Then, one would typically assign an edge between node i and node j , or one between i , j and k , if the corresponding element of $a_i^{(1)}$ or $a_i^{(2)}$ is greater than 0. However, the presence of higher-order interactions introduces significant sensitivity to noise [27], even when a 2-norm penalty is employed, as formulated in Eq. 12. To mitigate this issue, we define adaptive thresholds $\Delta_i^{(1)}$ for simple edges and $\Delta_i^{(2)}$ for 2-simplices, retaining only elements of $a_i^{(1)}$ and $a_i^{(2)}$ that exceed these thresholds. The thresholds are computed using a gap-based approach [50, 51]. Specifically, the elements of $a_i^{(1)}$ and $a_i^{(2)}$ are sorted in non-increasing order. Next, the gap between consecutive elements in each sorted vector is measured, weighted by the ratio of the same consecutive elements. Finally, the threshold values are determined by selecting the largest weighted gap, ensuring robustness against noise while preserving essential structural information [48]. In formulae,

$$\Delta_i^{(d)} = \arg \max_h \left(\frac{a'_{i,h}{}^{(d)}}{a'_{i,h+1}{}^{(d)}} \left(a'_{i,h}{}^{(d)} - a'_{i,h+1}{}^{(d)} \right) \right), \quad (13)$$

where d is the dimension of the simplices (1 or 2), and $a'_i{}^{(1)}$ and $a'_i{}^{(2)}$ are the sorted versions of $a_i^{(1)}$ and $a_i^{(2)}$. Finally, to prevent inconsistencies in the reconstructed simplicial complex, we drop any 2-simplex (i, j, k) if any edge (i, j) , (i, k) or (j, k) is missing from the network.

C. Global estimator

Even when eliminating simplicial inconsistencies, the PBP can still lead to reconstruction errors, because of the

independence of the estimates of different nodes. Thus, for example, the edge (i, j) , corresponding to the element $A_{i,j}^{(1)}$, may end up being included in the network, while the edge (j, i) , corresponding to the element $A_{j,i}^{(1)}$, is excluded, which would be inconsistent with the fact that the simplicial complex being reconstructed is undirected, and, as such, it must satisfy

$$A_{i,j}^{(1)} = A_{j,i}^{(1)}. \quad (14)$$

The situation quickly becomes more complex with 2-simplices, where the constraints to be satisfied are

$$A_{i,j,k}^{(2)} = A_{i,k,j}^{(2)} = A_{j,i,k}^{(2)} = A_{j,k,i}^{(2)} = A_{k,i,j}^{(2)} = A_{k,j,i}^{(2)}. \quad (15)$$

To address the limitations of PBP, the global estimator (GLO) reconstructs the network by solving all equations simultaneously while enforcing structural constraints [30]. Unlike local approaches that estimate each node independently, the global estimator treats the entire network as a coupled system [36, 52]. This method formulates network reconstruction as a large-scale optimization problem [53], where the adjacency matrix is inferred by minimizing discrepancies between observed dynamical data and predicted interactions [43, 54, 55]. To do so, we first introduce compressed flattenings of $\mathbf{A}^{(1)}$ and $\mathbf{A}^{(2)}$, which exclude any element on any diagonal and include

only the upper triangle and the uppermost pyramid, respectively, so that

$$\hat{A}^{(1)} = \left(A_{1,2}^{(1)}, A_{1,3}^{(1)}, \dots, A_{1,N}^{(1)}, A_{2,3}^{(1)}, \dots, A_{N-1,N}^{(1)} \right)^T \quad (16)$$

and

$$\hat{A}^{(2)} = \left(A_{1,2,3}^{(2)}, A_{1,2,4}^{(2)}, \dots, A_{1,2,N}^{(2)}, A_{1,3,4}^{(2)}, \dots, A_{N-2,N-1,N}^{(2)} \right)^T. \quad (17)$$

Then, we use these to build the vector of unknowns \hat{A} ,

$$\hat{A} = \left(\left(\hat{A}^{(1)} \right)^T, \left(\hat{A}^{(2)} \right)^T \right)^T, \quad (18)$$

which implicitly contains all the needed symmetry constraints.

Next, we carry out a similar procedure on the Π_i and the Φ_i . This results in the vectors

$$\begin{aligned} \hat{\Pi} &= \left(\hat{\Pi}_{t_1}, \hat{\Pi}_{t_2}, \dots, \hat{\Pi}_{t_M} \right)^T \\ &= \left(\pi_1(t_1), \pi_2(t_1), \dots, \pi_N(t_1), \pi_1(t_2), \dots, \pi_N(t_M) \right)^T \end{aligned} \quad (19)$$

and

$$\hat{\Phi} = \left(\hat{\Phi}_{t_1}, \hat{\Phi}_{t_2}, \dots, \hat{\Phi}_{t_M} \right)^T. \quad (20)$$

In the equation below,

$$\hat{\Phi}_{t_m} = \begin{pmatrix} C_{1,2,1}^{(1)}(t_m) & C_{1,2,2}^{(1)}(t_m) & \cdots & C_{1,2,N}^{(1)}(t_m) \\ C_{1,3,1}^{(1)}(t_m) & C_{1,3,2}^{(1)}(t_m) & \cdots & C_{1,3,N}^{(1)}(t_m) \\ \vdots & \vdots & \ddots & \vdots \\ C_{1,N,1}^{(1)}(t_m) & C_{1,N,2}^{(1)}(t_m) & \cdots & C_{1,N,N}^{(1)}(t_m) \\ C_{2,3,1}^{(1)}(t_m) & C_{2,3,2}^{(1)}(t_m) & \cdots & C_{2,3,N}^{(1)}(t_m) \\ \vdots & \vdots & \ddots & \vdots \\ C_{N-1,N,1}^{(1)}(t_m) & C_{N-1,N,2}^{(1)}(t_m) & \cdots & C_{N-1,N,N}^{(1)}(t_m) \\ C_{1,2,3,1}^{(2)}(t_m) & C_{1,2,3,2}^{(2)}(t_m) & \cdots & C_{1,2,3,N}^{(2)}(t_m) \\ C_{1,2,4,1}^{(2)}(t_m) & C_{1,2,4,2}^{(2)}(t_m) & \cdots & C_{1,2,4,N}^{(2)}(t_m) \\ \vdots & \vdots & \ddots & \vdots \\ C_{1,2,N,1}^{(2)}(t_m) & C_{1,2,N,2}^{(2)}(t_m) & \cdots & C_{1,2,N,N}^{(2)}(t_m) \\ C_{1,3,4,1}^{(2)}(t_m) & C_{1,3,4,2}^{(2)}(t_m) & \cdots & C_{1,3,4,N}^{(2)}(t_m) \\ \vdots & \vdots & \ddots & \vdots \\ C_{N-2,N-1,N,1}^{(2)}(t_m) & C_{N-2,N-1,N,2}^{(2)}(t_m) & \cdots & C_{N-2,N-1,N,N}^{(2)}(t_m) \end{pmatrix}, \quad (21)$$

where

$$C_{i,j,n}^{(1)}(t_m) = \begin{cases} P_{i,j}^{(1)}(t_m) & \text{if } n = i \\ P_{j,i}^{(1)}(t_m) & \text{if } n = j \\ 0 & \text{otherwise} \end{cases} \quad (22)$$

and

$$C_{i,j,k,n}^{(2)}(t_m) = \begin{cases} P_{i,j,k}^{(2)}(t_m) & \text{if } n = i \\ P_{j,i,k}^{(2)}(t_m) & \text{if } n = j \\ P_{k,i,j}^{(2)}(t_m) & \text{if } n = k \\ 0 & \text{otherwise.} \end{cases} \quad (23)$$

With this formalism, it is now possible to conduct a one-shot optimization of the entire network structure, aiming to find the solution given by

$$\arg \min_{\{\hat{A}\} | \hat{\Pi} = \hat{\Phi} \cdot \hat{A}} \left(\left\| \hat{A} \right\|_1 + \left\| \hat{\Pi} - \hat{\Phi} \cdot \hat{A} \right\|_2 \right). \quad (24)$$

Thus, this method represents a global estimator (GLO).

After estimating \hat{A} , we then sort $\hat{A}^{(1)}$ and $\hat{A}^{(2)}$ and determine the two global thresholds $\hat{\Delta}^{(1)}$ and $\hat{\Delta}^{(2)}$, using the same function as in Eq. 13, and delete all reconstructed edges whose corresponding element is smaller than or equal to the appropriate threshold. Finally, we delete any 2-simplex that has at least one missing 1-simplex on its constituent nodes, to guarantee that the reconstructed simplicial complex is consistent.

D. Global estimator with simplicial constraints

Our last method extends the global estimator to include an additional set of simplicial constraints (GLOC). Specifically, we maintain the formalism of GLO, but add the requirement that the value of the element of $\hat{A}^{(2)}$ corresponding to a 2-simplex be bounded from above individually by the three values of the elements of $\hat{A}^{(1)}$ corresponding to the 1-simplices on the same nodes, and that all be less than or equal to 1. This guarantees that a 2-simplex that is highly likely to exist implies 1-simplices on the same nodes that are at least as likely to be there. In fact, in the limiting case that an edge (i, j, k) exists for sure, all three edges (i, j) , (i, k) and (j, k) will certainly exist as well. The solution to find can then be written as

$$\arg \min_{\{\hat{A}\} | \hat{\Pi} = \hat{\Phi} \cdot \hat{A}} \left(\left\| \hat{A} \right\|_1 + \left\| \hat{\Pi} - \hat{\Phi} \cdot \hat{A} \right\|_2 \right). \quad (25)$$

$$A_{i,j,k}^{(2)} \leq A_{i,j}^{(1)} \leq 1$$

$$A_{i,j,k}^{(2)} \leq A_{i,k}^{(1)} \leq 1$$

$$A_{i,j,k}^{(2)} \leq A_{j,k}^{(1)} \leq 1$$

After solving the problem numerically, we still carry out the thresholding procedure as described above. As this can introduce structural inconsistencies, we also check for 2-simplices with missing induced 1-simplices and delete any we find, as in the previous methods.

IV. NETWORK CONSTRUCTION AND PERFORMANCE METRICS

To validate our methods, we conduct numerical simulations on three different types of synthetic complexes and on three complexes extracted from empirical data. Note that the structure of these complexes is used to advance the evolutionary games, but no information about it takes part in the reconstruction process.

A. Synthetic complexes

1. Non-preferential attachment model (NPA)

To build a simplicial complex in which the construction process does not include any bias, we follow the procedure outlined in Ref. [56]. Starting from an initial kernel of $N_0 = 5$ fully-connected nodes, we grow the complex by adding one node at each time step t . When a new node is added, m_{tri} existing edges are randomly extracted, and the new node is linked to the nodes that form them. Note that if $m_{\text{tri}} > 1$, we choose the links without any pairwise adjacency, so that the total number of nodes to which the new one is to be linked is always $2m_{\text{tri}}$. Following this procedure, at time t each edge has the same probability $p = \left[\frac{N_0(N_0-1)}{2} + 2m_{\text{tri}}(t-1) \right]^{-1}$ to be extracted. Thus, no preferential attachment takes place in this model. After reaching the desired number of nodes N , we take a fraction ρ of all triangles and add 2-simplices on the nodes that form them.

2. Preferential attachment model (PA)

To create complexes in which the growth process follows a preferential attachment rule, we change the probability distribution of the edges selected for linking the new node from uniform to one that is proportional to the number of triangles that each link is part of. Thus, the probability of extracting the edge (i, j) is $p_{ij} = \frac{k_{ij}}{\sum_{(i,j)} k_{ij}}$, where k_{ij} is the number of triangles that edge (i, j) participates in, and the sum is on all edges currently in the network. Note that the quantities in the previous formula depend on the time step, and we have avoided explicitly writing this dependence to reduce clutter. Also in this case, upon reaching the target size, we extract a random fraction ρ of triangles and add 2-simplices on their nodes.

3. Mixed model (MIX)

The two models above can be further integrated and generalized into a mixed one, which allows one to tune the power-law exponents of the resulting degree distributions for simple edges and 2-simplices [56]. To achieve this, we turn the probability of selecting the edge (i, j) into $p_{ij} = \left(1 - \frac{3}{2}B\right) \left[\frac{N_0(N_0-1)}{2} + 2m_{\text{tri}}(t-1) \right]^{-1} + B \frac{k_{ij}}{\sum_{(i,j)} k_{ij}}$. Here, the coefficient B is allowed to vary between 0 and 2, and it is worth noticing that the model reduces to NPA and PA for $B = 0$ and $B = \frac{2}{3}$, respectively. As in the previous two models, once the network has N nodes, we add 2-simplices on the nodes that form a fraction ρ of all the triangles.

B. Empirical complexes

To demonstrate the applicability of our reconstruction methods, we also use simplicial complexes inferred from real-world data. Specifically, we consider the network of social contacts recorded in a rural village in Malawi (Malawi) [57], the high-resolution data of face-to-face contacts during a scientific conference (SFHH) [58] and the interactions between patients and healthcare workers over a period of 96 hours in a non-emergency unit of a hospital in Lyon (LH10) [59]. To build a simplicial complex from each of the data sets, we first generate a weighted network in which the weights correspond to the total number of observed interactions between node pairs. Then, we delete all edges with a weight smaller than or equal to a threshold ζ and restrict ourselves to the unweighted version of the resulting largest connected component. The values we use for the threshold are 35 for Malawi, 55 for SFHH and 60 for LH10, resulting in networks of 50, 54 and 49 nodes, respectively. Finally, we split the data into 5-minute time windows. Any three nodes that form a triangle in any temporal window are turned into a 2-simplex.

C. Reconstruction and performance metrics

To evaluate the performance of our methods in reconstructing the networks, we use several metrics, based on the number of edges that are correctly or incorrectly detected. To define them, we start by calling TP the number of true positives, i.e., the number of existing edges that are determined. We also indicate with FP the number of false positives, which are edges that are incorrectly identified to exist. We use TN for the number of true negatives, which are missing edges that are correctly detected not to exist. Finally, FN is the number of false negatives, which are edges that are present in the network, but that a method fails to detect. Note that, the sum of these four values is the total possible number of edges E :

$$\begin{aligned} TP + TN + FP + FN &= E \\ &= \begin{cases} \binom{N}{2} = \frac{N(N-1)}{2} & \text{for 1-simplices} \\ \binom{N}{3} = \frac{N(N-1)(N-2)}{6} & \text{for 2-simplices.} \end{cases} \end{aligned} \quad (26)$$

Then, we evaluate the results using accuracy (ACC), true positive rate (TPR), positive predictive value (PPV), true negative rate (TNR) and F_1 score, which are de-

finied as follows:

$$ACC = \frac{TP + TN}{E}, \quad (27)$$

$$TPR = \frac{TP}{TP + FN}, \quad (28)$$

$$PPV = \frac{TP}{TP + FP}, \quad (29)$$

$$TNR = \frac{TN}{TN + FP}, \quad (30)$$

$$F_1 = \frac{2TP}{2TP + FP + FN}. \quad (31)$$

The range of all these quantities is between 0 and 1, with larger values indicating a better performance. Additionally, we consider the Matthews correlation coefficient (MCC), defined as

$$MCC = \frac{TP \cdot TN - FP \cdot FN}{\sqrt{(TN + FN)(TN + FP)(TP + FP)(TP + FN)}}, \quad (32)$$

whose range is $[-1, 1]$.

Furthermore, using the false positive rate

$$FPR = \frac{FP}{FP + TN}, \quad (33)$$

the recall rate

$$R = \frac{TP}{TP + FN}, \quad (34)$$

and the precision rate

$$P = \frac{TP}{TP + FP}, \quad (35)$$

we can define the receiver operating characteristic and the precision-recall curve. The former expresses how the TPR changes as a function of the FPR, and the latter how precision decreases as recall increases. Typically, the area under these curves is computed, and used as a measure of the classification performance of a method, with values closer to the theoretical maximum of 1 signifying better performance. Note that, in our case, the results of the method do not depend on a variable parameter. Thus, the areas under these curves can be computed analytically, so that the one under their ROC curve is

$$AUROC = \frac{1}{2} \left(\frac{TN}{FP + TN} + \frac{TP}{TP + FN} \right) \quad (36)$$

and the one under the precision-recall curve is

$$AUPR = \frac{1}{2} \frac{TP(2TP + FP + FN)}{(TP + FP)(TP + FN)}. \quad (37)$$

V. NUMERICAL RESULTS

A. Synthetic complexes

For our simulations, we use the synthetic models described in Subsection IV A, with $N = 50$ nodes and

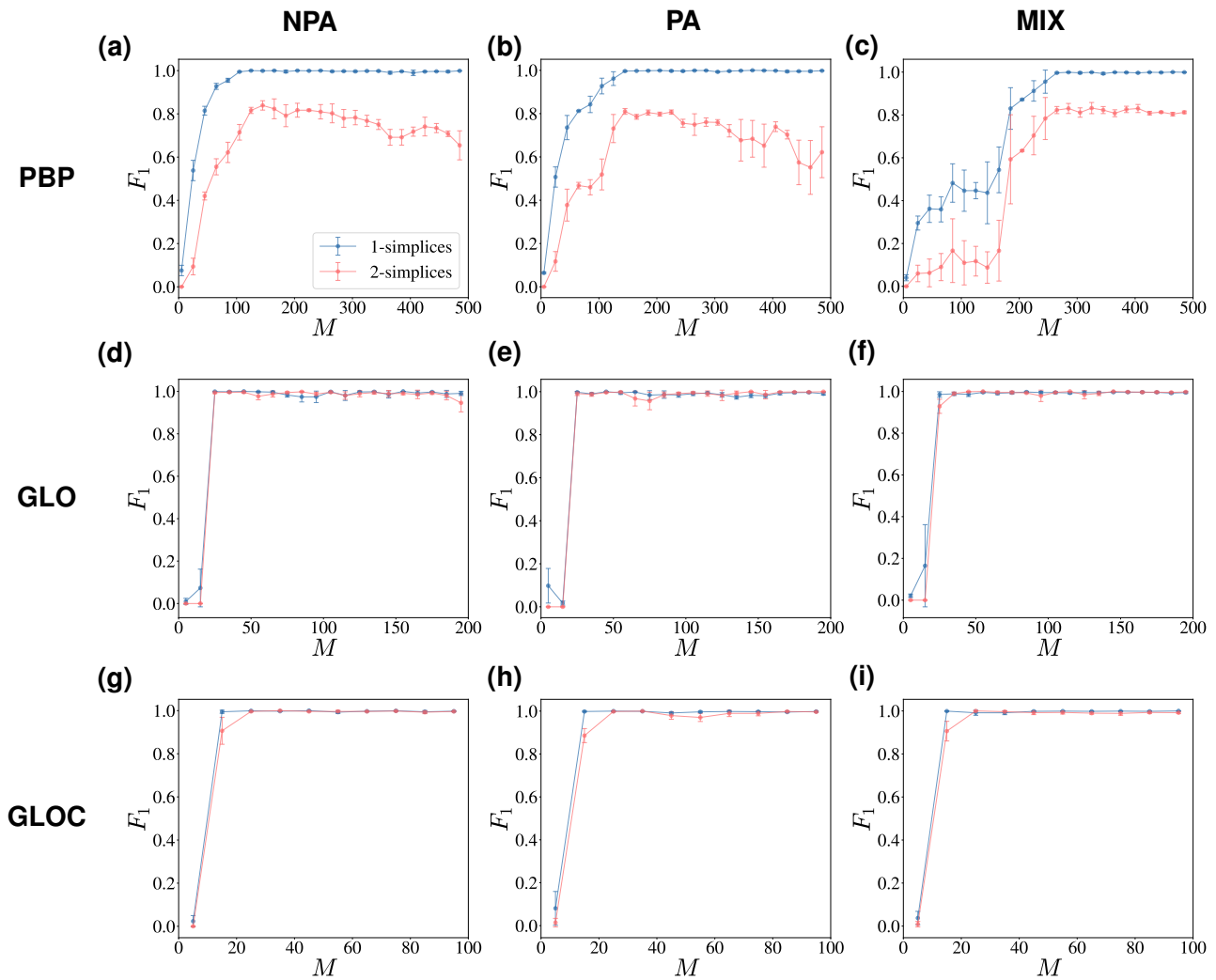


Figure 2. **Global reconstruction methods outperform PBP.** All three methods reach the highest possible value of the F_1 score for the reconstruction of 1-simplices (blue) playing the Prisoner’s Dilemma game for large enough sizes M of the observation sets. However, the score of PBP for 2-simplices (red) never increases above 0.8. At the same time, GLO and GLOC require fewer than 30 observations to reach a score of 1.

$\rho = 0.5$. For the MIX model, we put $B = 2$. In terms of the evolutionary games, we set $T = 1.3$ and $S = -0.4$ for the Prisoner’s Dilemma, $T = 1.3$ and $S = 0.4$ for the Snowdrift game, $T = 0.7$ and $S = -0.3$ for the Stag Hunt game, and $T = 0.7$ and $S = 0.3$ for the Harmony game. For the additional parameters of the three-body games, we put $G = \frac{3}{5}(T + S)$ and $W = \frac{2}{5}(T + S)$. Then, the payoff matrix and the strategy matrix are recorded for 500 rounds during five independent realization. Note that the strategies do not converge to an equilibrium within this number of rounds, because of the update process we use.

The reconstruction results for the synthetic simplicial complexes are detailed in Table S1 of the Supplementary Material. For all four games, all three methods provide very reliable reconstructions, with the accuracy always very close to 1. The two global estimators, however, al-

ways perform better than PBP, especially when comparing more sensitive metrics, such as the MCC and the F_1 score. The superiority of GLO and GLOC over PBP is even more evident in the reconstruction of 2-simplices, for which the differences in the complex metrics between the methods are larger.

To verify how the performance of the methods changes with the size of the observation set, we measured the F_1 score for different values of M . As shown in Fig. 2 for the Prisoner’s Dilemma, all three methods reach a high score for 1-simplices when M is large enough. The difference between them lies in their performance on 2-simplices, for which the highest value that PBP achieves is never above 0.8, and often with a large statistical uncertainty. This indicates that the reconstructions provided by PBP cannot be improved beyond a certain quality by indefinitely increasing the number of observations.

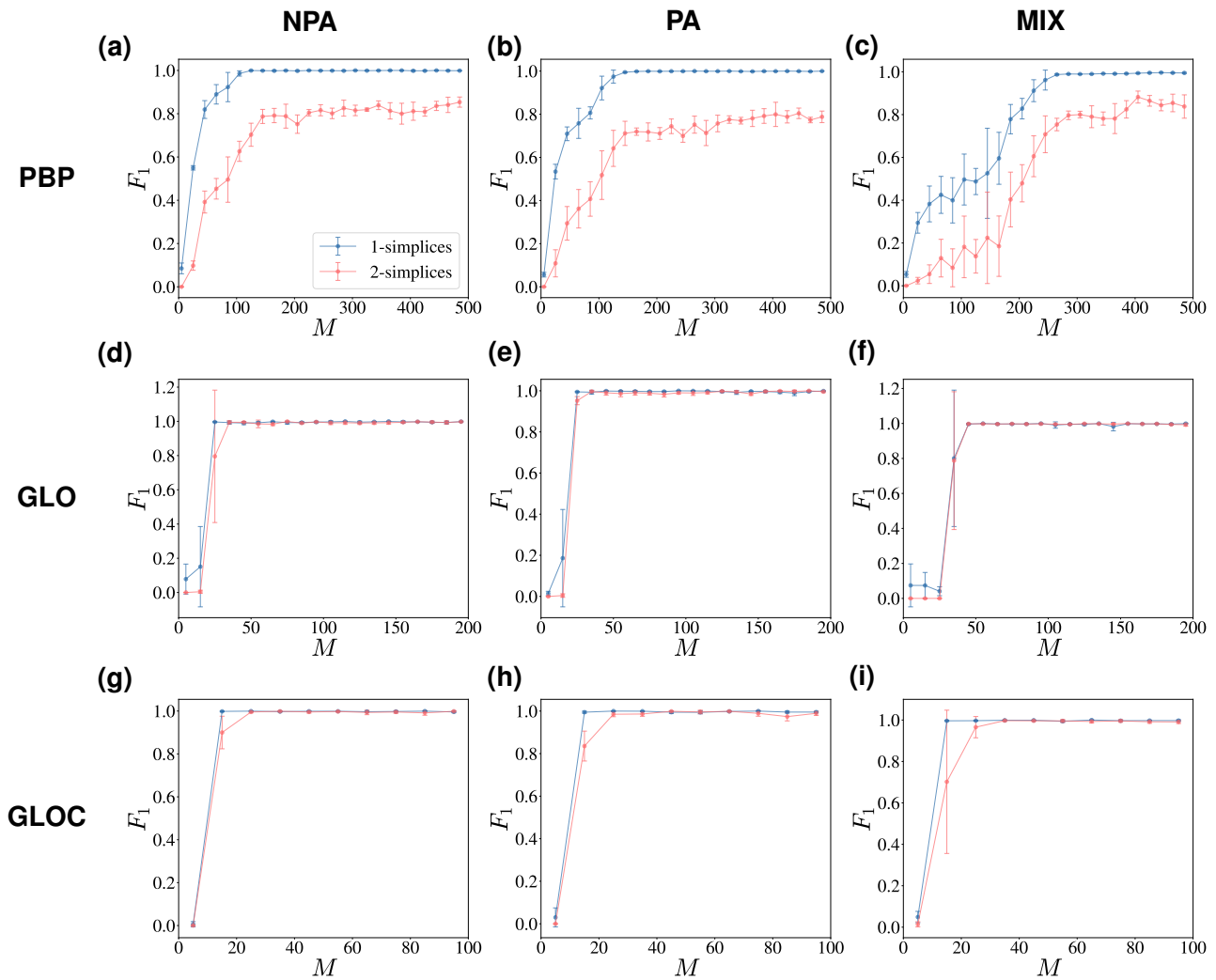


Figure 3. **GLOC requires the smallest minimum observation set for noisy data.** The relative performance of all three methods on noisy data ($q = 1\%$) from a Prisoner's Dilemma game is unchanged with respect to the noiseless case (Fig. 2). However, the minimum size of the observation set M needed to achieve a high F_1 score is higher than the one needed in the absence of noise, particularly for 2-simplices (red) in the MIX model. Also, this increase is the smallest for GLOC, making it the best of the three methods when data are affected by noise.

Conversely, both GLO and GLOC reach a score of 1 for all models with fewer than 30 observations.

B. Synthetic complexes with noise

In real-world situations, empirical measurements in transient phases can be affected by different types of errors and uncertainties, leading to further challenges to reconstruct the topology of networks. To examine how perturbations affect the reliability of our methods, we tested them on "noisy" data using two different noise injection approaches. In one aspect, we created the noise of payoffs by adding a random value ε to each element of the measured payoff matrix $\mathbf{\Pi}$. Specifically, ε was extracted from a normal distribution with 0 mean and standard

deviation $\sigma = q\sigma_{\Pi}$, where σ_{Π} is the standard deviation of the distribution of elements of the unperturbed payoff matrix. Additionally, we incorporated flipping noise by inverting each element of the strategy matrix \mathbf{S} with a probability ψ , simulating errors in empirical observations of strategies. This dual noise modeling allows us to provide a more comprehensive assessment of robustness beyond equilibrium states.

The reconstruction results for complexes with noise in payoffs, detailed in Table S2 of the Supplementary Material, show that small amounts of noise ($q = 1\%$) do not significantly affect the accuracy of the methods, or their overall performance. However, differences between PBP, GLO and GLOC become more apparent when the amount of noise is increased to $q = 5\%$. In that case, and even for 1-simplices, only GLOC maintains high values

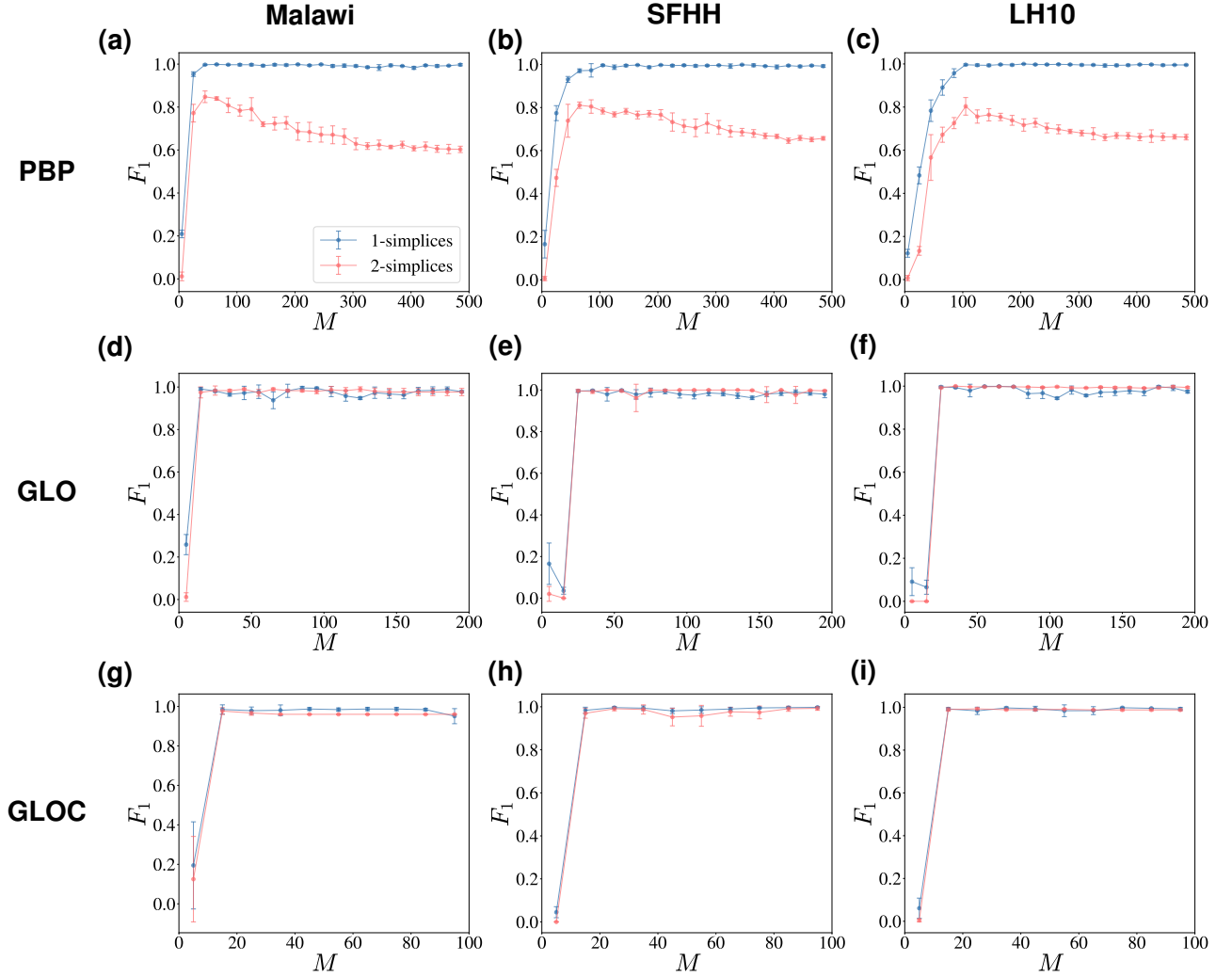


Figure 4. **GLO and GLOC outperform PBP on empirical complexes.** On empirical simplicial complexes, all three methods reach the highest possible value of the F_1 score for the reconstruction of 1-simplices (blue) playing the Prisoner’s Dilemma game for large enough sizes M of the observation sets. However, the score of PBP (red) never increases above 0.85 for 2-simplices.

across the metrics. Indeed, GLOC consistently achieves the highest scores for 2-simplices as well, demonstrating its superiority in reconstructing higher-order interactions regardless of the level of noise. Further analysis of strategy contamination noise, as shown in Table S3 of the Supplementary Material, reveals that GLOC remains the most robust method, even when the observed strategies are corrupted by flipping errors. While all methods, especially GLO, experience performance degradation due to noise in strategies, GLOC still retains a significant advantage over PBP and GLO.

The presence of noise also affects the minimum number of required observations to achieve a high-quality reconstruction. In fact, when noises in payoffs are emphasized (Fig. 3), the minimum size of the observation data set needed to obtain an F_1 score of at least 0.8 for 2-simplices increases, with respect to noiseless data, even

if the noise factor is only 1%. When the noise originates from strategy contamination (Fig. S1 of the Supplementary Material), the performance of GLO drops and fluctuates significantly across all three synthetic networks, with large error bars indicating high sensitivity to noisy strategies. PBP, while more stable, exhibits a slight increase in F_1 scores with additional observations. In contrast, GLOC achieves superior performance with far fewer observations, reaching an $F_1 \geq 0.4$ much earlier than the other methods. These results demonstrate the necessity of having larger data sets for effective higher-order network reconstruction, especially in the presence of noise. Notably, GLOC requires the fewest additional observations while maintaining a strong overall performance, confirming that the method is appropriate for higher-order interactions even in noisy environments, and highlighting its robustness.

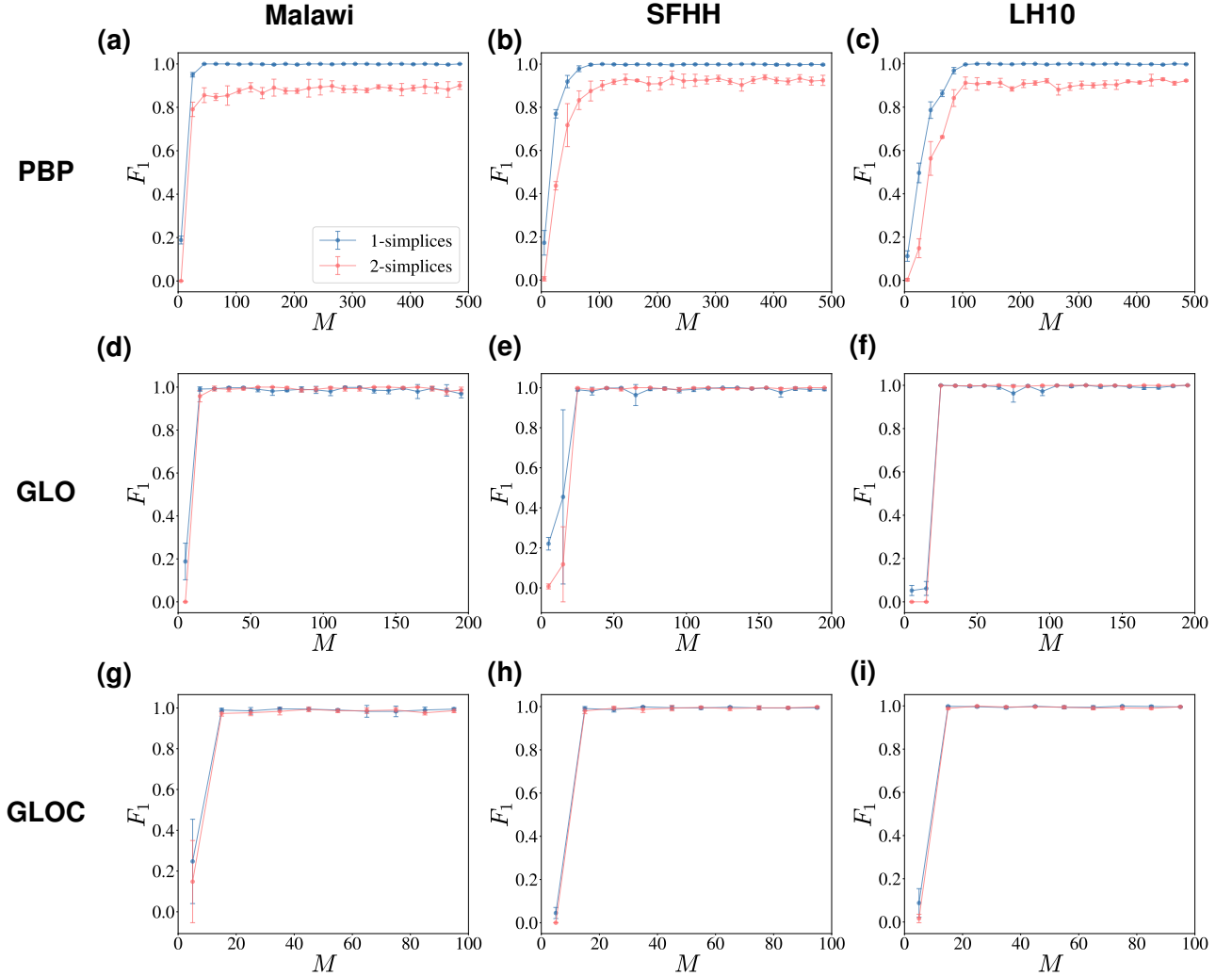


Figure 5. **GLOC is the best performing method to reconstruct empirical complexes with contaminated payoffs.** On empirical simplicial complexes, the relative performance of all three methods on noisy data ($q = 1\%$) from a Prisoner’s Dilemma game is the same as that of the noiseless case (Fig. 4). However, GLO and GLOC require the smallest data sets to achieve a high score. Moreover, the error bars for GLOC results are smaller than those for GLO, indicating that it is more robust to noise.

C. Empirical complexes

To validate the general applicability of our methods, we further test them on empirical simplicial complexes. Specifically, we build the complexes from the Malawi, SFHH and LH10 data sets, as described in Subsection IV B, and reconstruct the networks from observations of the Prisoner’s Dilemma game.

The values of the metrics for our reconstructions are reported in Table S4 and S5 of the Supplementary Material. When noise is introduced in the payoff matrix, all of three methods perform well in reconstructing 1-simplices. However, GLO and GLOC consistently outperform PBP in 2-simplex reconstruction, demonstrating their superior ability to capture higher-order interactions. After the addition of noise in payoffs, the difference in performance

is amplified, and GLOC remains the only method that maintains high scores for all metrics. Performance differences become more pronounced when noise contaminates the information of strategies. As seen in Table S5, despite the notable performance declines that all of three methods suffer under small perturbations in strategy observations ($\psi = 1\%$), GLOC still reaches the highest F_1 scores to reconstruct 2-simplices. These results highlight GLOC’s robustness and superiority, ensuring high accuracy even when empirical data is subject to fluctuations and uncertainty during transient phases.

Measurements of the F_1 score for different sizes of the observation set are shown in Fig. 4 and in Fig. 5 in the absence and in the presence of noise regarding payoffs, respectively. In all cases, and consistently with the results obtained on synthetic complexes, GLOC is

the method that requires the smallest number of observations M to reach a high quality of reconstruction, on both 1-simplices and 2-simplices. In fact, the number of required observations is only around 15, which is an even smaller value than the one needed for synthetic simplicial complexes. As illustrated in Fig. S2 the impact on reconstruction further varies across methods when strategy noise ($\psi = 1\%$) is introduced. PBP, while relatively stable, requires a large number of observations to reach a reasonable F_1 score. GLO, on the other hand, shows extreme variability, with large fluctuations and poor performance across different network types, indicating its sensitivity to erroneous strategies. In contrast, GLOC remains the most reliable method, where highest F_1 scores can be guaranteed within the smallest observation data sets. The robustness of GLOC against noise highlights its effectiveness in reconstructing simplicial complexes using data captured exclusively during the transient phase of evolutionary game dynamics, rather than relying on equilibrium states. This capability is particularly valuable in real-world scenarios where networked interactions evolve dynamically, and equilibrium conditions are rarely observed. Moreover, GLOC's ability to maintain relatively high accuracy with limited, noisy data suggests that it can significantly reduce the amount of data collected in scenarios where resources are limited and where data contamination is unavoidable during collection.

VI. CONCLUSIONS

In summary, we have introduced three methods for the reconstruction of simplicial complexes. One is a local point-by-point estimator (PBP), and the other two are a global approach (GLO) and a global estimator which explicitly includes simplicial constraints (GLOC). These are amongst the very few approaches that can reconstruct higher-order networks using observations of evolutionary dynamics in transient phases. All three methods perform well according to a number of different metrics when accounting for the reconstructed simple edges. However, while still obtaining high-quality results, PBP does not provide a perfect accuracy when measuring the reconstructed 2-simplices. In this latter case, GLO and GLOC furnish more precise results, with GLOC being particularly useful in the case of noisy data. Additionally, GLOC achieves highly precise results with significantly fewer observations, regardless of whether the payoff information is contaminated or the strategies deviate from equilibrium due to noise.

These characteristics of the behaviour of the methods are independent of the origin of the network being reconstructed. In fact, the superiority of GLOC remains unchanged whether different methods are applied to syn-

thetic models of simplicial complexes, or to higher-order structures derived from empirical data.

This suggests several considerations about those scenarios where each of the three methods is the most appropriate for being used. For instance, in situations where data collection is not an expensive task, and where a very high quality of reconstruction of higher-order interactions, yet short of perfection, is acceptable, PBP would be the method of choice, as it is computationally less complex, with the cost of requiring more observation data. If, instead the reconstruction quality is of absolute importance, or if the costs associated to the process of data gathering are higher than those related to computing time, GLO is the best choice. However, if one cannot be sure that the uncertainties on the data are negligible, while still requiring the best possible reconstruction regardless of the complexity of the task, then GLOC is the method to use. Our methods are rooted in mathematical optimization, providing a flexible and adaptive framework for reconstructing higher-order structures in real-world distributed systems, where equilibrium is often impractical due to the dynamic and fluctuating nature of interactions. By leveraging transient-phase data rather than relying on equilibrium states, our approach offers a more realistic and effective solution for studying higher-order interactions within simplicial complexes. This framework fills a critical methodological gap by systematically addressing the challenges of reconstructing higher-order evolutionary game dynamics, a perspective that has not been thoroughly explored in previous research. Furthermore, our suite of optimization-based methods allows for tailored reconstruction strategies depending on specific system requirements, while avoiding the intrinsic limitations of traditional statistical techniques that often assume stationarity or long-term convergence.

ACKNOWLEDGMENTS

Y.M. and Z.J. acknowledge partial support from the National Natural Science Foundation of China (No. 72171084 and No. 91746108) and the China Scholar Council State Scholarship Fund (No. 202306740033). F.F. acknowledges partial support from the China Scholar Council State Scholarship Fund (No. 202306830151). C.I.D.G. acknowledges funding from the Bulgarian Ministry of Education and Science, under project number BG-RRP-2.004-0006-C02. S.B. acknowledges support from the project n.PGR01177 "Systems with higher order interactions and fractional derivatives for applications to AI and high performance computing" of the Italian Ministry of Foreign Affairs and International Cooperation.

[1] R. Albert and A.-L. Barabási, *Rev. Mod. Phys.* **74**, 47 (2002).

[2] S. Boccaletti *et al.*, *Phys. Rep.* **424**, 175 (2006).

- [3] S. Boccaletti *et al.*, Phys. Rep. **544**, 1 (2014).
- [4] D. Papo, M. Zanin, J. A. Pineta-Pardo, S. Boccaletti and J. M. Buldu, Philos. T. Roy. Soc. B **369**, 20130525 (2014).
- [5] K. L. Mine *et al.*, Nat. Commun. **4**, 1806 (2013).
- [6] S. Treviso III, A. Nyberg, C. I. del Genio and K. E. Bassler, J. Stat. Mech. – Theory E., P02003 (2015).
- [7] F. Botta and C. I. del Genio, J. Stat. Mech. – Theory E., 123402 (2016).
- [8] F. Botta and C. I. del Genio, PLoS One **12** (3), e0174198 (2017).
- [9] C. A. Hill *et al.*, Nat. Neurosci. **20**, 1142 (2017).
- [10] M. Perc *et al.*, Phys. Rep. **687**, 1 (2017).
- [11] X. Li *et al.*, Proc. Natl. Acad. Sci. USA **115**, 30 (2018).
- [12] Z. Wang *et al.*, Nat. Commun. **9**, 2954 (2018).
- [13] L. Schmid, K. Chatterjee, C. Hilbe and M. A. Nowak, Nat. Hum. Behav. **5**, 1292 (2021).
- [14] E. Connelly, C. I. del Genio and E. Harrison, mBio **11**, e03136 (2020).
- [15] E. Connelly, C. Lee, J. Furner-Pardoe, C. I. del Genio and E. Harrison, Patterns **3**, 100362 (2022).
- [16] C. I. del Genio and T. House, Phys. Rev. E **88**, 040801(R) (2013).
- [17] Z.-K. Zhang *et al.*, Phys. Rep. **651**, 1 (2016).
- [18] X. Zhang *et al.*, Nat. Commun. **13**, 6218 (2022).
- [19] C. I. del Genio and T. Gross, New J. Phys. **13**, 103038 (2011).
- [20] C. I. del Genio, M. Romance, R. Criado and S. Boccaletti, Phys. Rev. E **92**, 062819 (2015).
- [21] C. I. del Genio, J. Gómez-Gardeñes, I. Bonamassa and S. Boccaletti, Sci. Adv. **2**, e1601679 (2016).
- [22] C. I. del Genio, S. Faci-Lazaro, J. Gómez-Gardeñes and S. Boccaletti, Commun. Phys. **5**, 121 (2022).
- [23] S. Boccaletti *et al.*, Phys. Rep. **1018**, 1 (2023).
- [24] M. Herrgård *et al.*, Nat. Biotechnol. **26**, 1155 (2008).
- [25] S. Chen, A. Shojaie and D. Witten, J. Am. Stat. Assoc. **112**, 1697 (2017).
- [26] J. Runge, Chaos **28**, 075310 (2018).
- [27] H. Wang, C. Ma, H.-S. Chen, Y.-C. Lai and H.-F. Zhang, Nat. Commun. **13**, 3043 (2022).
- [28] H.-C. Xu, Z.-Y. Wang, F. Jawadi and W.-X. Zhou, Chaos Soliton. Fract. **167**, 113031 (2023).
- [29] W.-X. Wang, Y.-C. Lai, C. Grebogi and J. Ye, Phys. Rev. X **1**, 021021 (2011).
- [30] Z. Hang, P. Dai, S. Jia and Z. Yu, Chaos Soliton. Fract. **139**, 110287 (2020).
- [31] K. Huang, Z. Wang and M. Jusup, IEEE Trans. Netw. Sci. Eng. **7**, 466 (2020).
- [32] J. Dai, K. Huang, Y. Liu, C. Yang and Z. Wang, IEEE Syst. J. **15**, 1959 (2021).
- [33] C. Ma, Y.-C. Lai, X. Li and H.-F. Zhang, Phys. Rev. E **108**, 034304 (2023).
- [34] T. Squartini, G. Caldarelli, G. Cimini, A. Gabrielli and D. Garlaschelli, Phys. Rep. **757**, 1 (2018).
- [35] C. I. del Genio, T. Gross and K. E. Bassler, Phys. Rev. Lett. **107**, 178701 (2011).
- [36] F. Malizia *et al.*, Nat. Commun. **15**, 5184 (2024).
- [37] H. Chiba-Okabe, J. Plotkin, Proc. Natl. Acad. Sci. USA **121** (49), e2414291121 (2024).
- [38] X. Han *et al.*, Chaos Soliton. Fract. **164**, 112684 (2022).
- [39] C. McIntosh *et al.*, J. Econ. Behav. Organ. **95**, 270 (2013).
- [40] A. Civilini, O. Sadekar, F. Battiston, J. Gomez-Gardenes and V. Latora, Phys. Rev. Lett. **132**, 167401 (2024).
- [41] R.-Q. Su, X. Ni, W.-X. Wang, and Y.-C. Lai, Phys. Rev. E **85**, 056220 (2012).
- [42] W.-X. Wang, Y.-C. Lai, and C. Grebogi, Phys. Rep. **644**, 1 (2016).
- [43] X. Han, Z. Shen, W.-X. Wang, and Z. Di, Phys. Rev. Lett. **114**, 028701 (2015).
- [44] M. K. S. Yeung, J. Tegnér, and J. J. Collins, Proc. Natl. Acad. Sci. USA **99**, 6163 (2002).
- [45] B.-B. Xiang, Z.-K. Bao, C. Ma, X. Zhang, H.-S. Chen, and H.-F. Zhang, Chaos **28**, 013122 (2018).
- [46] M. Timme, Phys. Rev. Lett. **98**, 224101 (2007).
- [47] Z. Shen, W.-X. Wang, Y. Fan, Z. Di, and Y.-C. Lai, Nat. Commun. **5**, 4323 (2014).
- [48] J. Li, Z. Shen, W.-X. Wang, C. Grebogi, and Y.-C. Lai, Phys. Rev. E **95**, 032303 (2017).
- [49] Y.-Z. Chen and Y.-C. Lai, Phys. Rev. E **97**, 032317 (2018).
- [50] C. Ma *et al.*, Phys. Rev. E **97**, 022301 (2018).
- [51] C. Ma, H. Wang, and H.-F. Zhang EPL **144**, 21002 (2023).
- [52] H.-Y. Gu *et al.*, Proc. Natl. Acad. Sci. USA **119** (33), e2201062119 (2022).
- [53] J. Liu *et al.*, Chaos Soliton. Fract. **173**, 113739 (2023).
- [54] S. L. Brunton *et al.*, Proc. Natl. Acad. Sci. USA **113** (15), 3932 (2016).
- [55] L. Shi *et al.*, Phys. Rev. Res. **3**, 043210 (2021).
- [56] K. Kovalenko *et al.*, Commun. Phys. **4**, 43 (2021).
- [57] L. Ozella *et al.*, EPJ Data Sci. **10**, 46 (2021).
- [58] M. Géniois and A. Barrat, EPJ Data Sci. **7**, 11 (2018).
- [59] P. Vanhems *et al.*, PLoS One **8** (9), e73970 (2013).

Reconstructing simplicial complexes from evolutionary games

Supplementary Material

Yin-Jie Ma,^{1,2,3} Zhi-Qiang Jiang,^{1,2,*} Fanshu Fang,^{3,4} Charo I. del Genio,^{5,6} and Stefano Boccaletti^{3,6,7,†}

¹*School of Business, East China University of Science and Technology, Shanghai, China*

²*Research Center for Econophysics, East China University of Science and Technology, Shanghai, China*

³*CNR - Institute of Complex Systems, Via Madonna del Piano 10, I-50019, Sesto Fiorentino, Italy*

⁴*College of Economics and Management, Nanjing University of Aeronautics and Astronautics, Nanjing, China*

⁵*Institute of Smart Agriculture for Safe and Functional Foods and Supplements, Trakia University, Stara Zagora 6000, Bulgaria*

⁶*Research Institute of Interdisciplinary Intelligent Science,
Ningbo University of Technology, 315104, Ningbo, China*

⁷*Sino-Europe Complexity Science Center, School of Mathematics,
North University of China, 030051, Taiyuan, China*

(Dated: March 21, 2025)

Method	ACC/TPR/PPV/TNR/ F_1 /MCC/AUROC/AUPR													
(Net type, Game type, d)	(NPA, PD, 1)							(NPA, PD, 2)						
PBP	0.99/0.96/1.00/1.00/0.98/0.97/0.98/0.98	1.00/0.92/0.51/1.00/0.64/0.67/0.96/0.71												
GLO	0.99/1.00/0.95/0.99/0.97/0.97/1.00/0.98	1.00/1.00/0.98/1.00/0.99/0.99/1.00/0.99												
GLOC	1.00/1.00/0.99/1.00/1.00/1.00/1.00/1.00	1.00/1.00/0.99/1.00/1.00/1.00/1.00/1.00												
(Net type, Game type, d)	(PA, PD, 1)							(PA, PD, 2)						
PBP	0.96/0.76/1.00/1.00/0.86/0.85/0.88/0.90	0.99/0.58/0.37/1.00/0.45/0.46/0.79/0.48												
GLO	1.00/1.00/0.97/0.99/0.98/0.98/1.00/0.98	1.00/1.00/0.98/1.00/0.99/0.99/1.00/0.99												
GLOC	1.00/1.00/1.00/1.00/1.00/1.00/1.00/1.00	1.00/1.00/0.99/1.00/1.00/1.00/1.00/1.00												
(Net type, Game type, d)	(MIX, PD, 1)							(MIX, PD, 2)						
PBP	0.89/0.26/1.00/1.00/0.41/0.48/0.63/0.69	0.99/0.04/0.39/1.00/0.07/0.12/0.52/0.22												
GLO	1.00/1.00/0.99/1.00/0.99/0.99/1.00/0.99	1.00/1.00/0.96/1.00/0.98/0.98/1.00/0.98												
GLOC	1.00/1.00/1.00/1.00/1.00/1.00/1.00/1.00	1.00/1.00/0.98/1.00/0.99/0.99/1.00/0.99												
(Net type, Game type, d)	(NPA, SD, 1)							(NPA, SD, 2)						
PBP	0.99/0.93/1.00/1.00/0.96/0.96/0.97/0.97	0.99/0.83/0.38/0.99/0.52/0.56/0.91/0.61												
GLO	1.00/1.00/0.99/1.00/0.99/0.99/1.00/0.99	1.00/1.00/1.00/1.00/1.00/1.00/1.00/1.00												
GLOC	1.00/1.00/0.98/1.00/0.99/0.99/1.00/0.99	1.00/1.00/0.97/1.00/0.98/0.98/1.00/0.98												
(Net type, Game type, d)	(PA, SD, 1)							(PA, SD, 2)						
PBP	0.96/0.74/1.00/1.00/0.85/0.84/0.87/0.89	0.99/0.59/0.32/0.99/0.41/0.43/0.79/0.45												
GLO	1.00/1.00/0.99/1.00/1.00/0.99/1.00/1.00	1.00/1.00/0.98/1.00/0.99/0.99/1.00/0.99												
GLOC	1.00/1.00/0.98/1.00/0.99/0.99/1.00/0.99	1.00/1.00/0.99/1.00/0.99/0.99/1.00/0.99												
(Net type, Game type, d)	(MIX, SD, 1)							(MIX, SD, 2)						
PBP	0.89/0.30/0.96/1.00/0.46/0.50/0.65/0.69	0.99/0.13/0.38/1.00/0.19/0.21/0.57/0.26												
GLO	1.00/1.00/0.99/1.00/1.00/1.00/1.00/1.00	1.00/1.00/0.96/1.00/0.98/0.98/1.00/0.98												
GLOC	1.00/1.00/0.99/1.00/1.00/1.00/1.00/1.00	1.00/1.00/0.99/1.00/1.00/1.00/1.00/1.00												
(Net type, Game type, d)	(NPA, SH, 1)							(NPA, SH, 2)						
PBP	0.99/0.97/1.00/1.00/0.98/0.98/0.98/0.98	0.99/0.96/0.47/1.00/0.63/0.67/0.98/0.71												
GLO	1.00/1.00/0.99/1.00/1.00/0.99/1.00/1.00	1.00/1.00/0.93/1.00/0.96/0.96/1.00/0.96												
GLOC	1.00/1.00/0.97/0.99/0.99/0.98/1.00/0.99	1.00/1.00/0.99/1.00/0.99/0.99/1.00/0.99												
(Net type, Game type, d)	(PA, SH, 1)							(PA, SH, 2)						
PBP	0.99/0.94/1.00/1.00/0.97/0.96/0.97/0.97	0.99/0.94/0.40/0.99/0.56/0.61/0.97/0.67												
GLO	1.00/1.00/1.00/1.00/1.00/1.00/1.00/1.00	1.00/1.00/1.00/1.00/1.00/1.00/1.00/1.00												
GLOC	1.00/1.00/1.00/1.00/1.00/1.00/1.00/1.00	1.00/1.00/0.99/1.00/0.99/0.99/1.00/0.99												
(Net type, Game type, d)	(MIX, SH, 1)							(MIX, SH, 2)						
PBP	0.90/0.36/0.99/1.00/0.52/0.56/0.68/0.72	0.99/0.09/0.31/1.00/0.14/0.16/0.55/0.20												
GLO	1.00/1.00/0.99/1.00/1.00/1.00/1.00/1.00	1.00/1.00/0.99/1.00/0.99/0.99/1.00/0.99												
GLOC	1.00/1.00/0.99/1.00/0.99/0.99/1.00/0.99	1.00/1.00/1.00/1.00/1.00/1.00/1.00/1.00												

* Corresponding author: zqjiang@ecust.edu.cn

† Corresponding author: stefano.boccaletti@gmail.com

(Net type, Game type, d)	(NPA, H, 1)	(NPA, H, 2)
PBP	0.99/0.91/1.00/1.00/0.95/0.95/0.96/0.96	1.00/0.82/0.62/1.00/0.70/0.71/0.91/0.72
GLO	1.00/1.00/1.00/1.00/1.00/1.00/1.00/1.00	1.00/0.99/1.00/1.00/0.99/0.99/0.99/0.99
GLOC	1.00/1.00/1.00/1.00/1.00/1.00/1.00/1.00	1.00/1.00/0.99/1.00/0.99/0.99/1.00/0.99
(Net type, Game type, d)	(PA, H, 1)	(PA, H, 2)
PBP	0.97/0.80/0.99/1.00/0.89/0.88/0.90/0.91	1.00/0.70/0.57/1.00/0.61/0.62/0.85/0.63
GLO	1.00/1.00/1.00/1.00/1.00/1.00/1.00/1.00	1.00/0.97/0.94/1.00/0.96/0.96/0.99/0.96
GLOC	1.00/1.00/1.00/1.00/1.00/1.00/1.00/1.00	1.00/1.00/0.97/1.00/0.98/0.98/1.00/0.98
(Net type, Game type, d)	(MIX, H, 1)	(MIX, H, 2)
PBP	0.89/0.29/1.00/1.00/0.44/0.50/0.64/0.70	0.99/0.10/0.33/1.00/0.15/0.17/0.55/0.21
GLO	1.00/1.00/0.99/0.99/0.99/0.99/1.00/1.00	1.00/0.65/0.98/1.00/0.65/0.67/0.83/0.82
GLOC	1.00/1.00/1.00/1.00/1.00/1.00/1.00/1.00	1.00/1.00/0.85/1.00/0.91/0.91/1.00/0.92

Table S1: **The GLO and GLOC methods perform better than PBP.** Values of accuracy (ACC), true positive rate (TPR), positive predictive value (PPV), true negative rate (TNR), F_1 score, Matthews correlation coefficient (MCC), as well as the area under the receiver operating characteristic curve (AUROC) and that under the precision-recall curve (AUPR) show that all three methods perform well in the reconstruction of 1-simplices. However, GLO and GLOC provide much better results on 2-simplices, especially according to more complex metrics. The results are reported by type of synthetic simplicial complex model (NPA, PA and MIX), type of evolutionary game (Prisoner’s Dilemma – PD, Snowdrift – SD, Stag Hunt – SH and Harmony – H), and dimension d of the simplices considered. In all cases, the number of nodes is 50, the number of observations is 95 and $\rho = 0.5$.

Method	ACC/TPR/PPV/TNR/ F_1 /MCC/AUROC/AUPR	
(Net type, q, d)	(NPA, 1%, 1)	(NPA, 1%, 2)
PBP	0.99/0.90/1.00/1.00/0.95/0.94/0.95/0.96	0.99/0.79/0.42/1.00/0.54/0.57/0.89/0.61
GLO	1.00/1.00/0.99/1.00/1.00/1.00/1.00/1.00	1.00/1.00/0.99/1.00/1.00/1.00/1.00/1.00
GLOC	1.00/1.00/0.99/1.00/1.00/1.00/1.00/1.00	1.00/1.00/1.00/1.00/1.00/1.00/1.00/1.00
(Net type, q, d)	(NPA, 5%, 1)	(NPA, 5%, 2)
PBP	0.98/0.89/1.00/1.00/0.94/0.93/0.95/0.95	0.99/0.78/0.37/0.99/0.50/0.53/0.89/0.58
GLO	1.00/1.00/0.98/1.00/0.99/0.99/1.00/0.99	1.00/0.96/0.99/1.00/0.98/0.98/0.98/0.98
GLOC	1.00/1.00/0.99/1.00/0.99/0.99/1.00/0.99	1.00/1.00/0.98/1.00/0.99/0.99/1.00/0.99
(Net type, q, d)	(PA, 1%, 1)	(PA, 1%, 2)
PBP	0.97/0.80/1.00/1.00/0.89/0.88/0.90/0.92	0.99/0.66/0.34/0.99/0.45/0.47/0.83/0.50
GLO	1.00/1.00/1.00/1.00/1.00/1.00/1.00/1.00	1.00/1.00/0.98/1.00/0.99/0.99/1.00/0.99
GLOC	1.00/1.00/0.99/1.00/1.00/0.99/1.00/1.00	1.00/1.00/0.98/1.00/0.99/0.99/1.00/0.99
(Net type, q, d)	(PA, 5%, 1)	(PA, 5%, 2)
PBP	0.96/0.77/1.00/1.00/0.87/0.86/0.88/0.90	0.99/0.64/0.35/0.99/0.45/0.47/0.82/0.49
GLO	0.91/0.41/0.98/1.00/0.41/0.45/0.70/0.74	1.00/0.26/0.60/1.00/0.30/0.20/0.63/0.63
GLOC	0.97/0.80/0.98/1.00/0.91/0.81/0.90/0.91	1.00/0.80/0.95/1.00/0.78/0.79/0.90/0.88
(Net type, q, d)	(MIX, 1%, 1)	(MIX, 1%, 2)
PBP	0.89/0.28/0.99/1.00/0.44/0.50/0.64/0.69	0.99/0.06/0.26/1.00/0.09/0.12/0.53/0.16
GLO	1.00/1.00/1.00/1.00/1.00/1.00/1.00/1.00	1.00/1.00/1.00/1.00/1.00/1.00/1.00/1.00
GLOC	1.00/1.00/0.99/1.00/1.00/1.00/1.00/1.00	1.00/1.00/1.00/1.00/1.00/0.99/1.00/0.99
(Net type, q, d)	(MIX, 5%, 1)	(MIX, 5%, 2)
PBP	0.88/0.23/0.97/1.00/0.37/0.43/0.62/0.66	0.99/0.06/0.15/1.00/0.08/0.09/0.53/0.11
GLO	0.85/0.02/1.00/1.00/0.05/0.14/0.51/0.59	0.99/0.00/0.00/1.00/0.00/UD/0.50/0.50
GLOC	0.91/0.38/1.00/1.00/0.41/0.46/0.69/0.74	1.00/0.35/0.58/1.00/0.37/UD/0.68/0.67

Table S2: **The GLOC method performs consistently better than PBP and GLO when the measured payoff matrix is contaminated by noise.** Values of accuracy (ACC), true positive rate (TPR), positive predictive value (PPV), true negative rate (TNR), F_1 score, Matthews correlation coefficient (MCC), as well as the area under the receiver operating characteristic curve (AUROC) and that under the precision-recall curve (AUPR) for noisy data from a Prisoner’s Dilemma game show that, while PBP and GLO are affected by higher levels of noise in payoffs, GLOC maintains high scores across the different metrics. The results are reported by type of synthetic simplicial complex model (NPA, PA and MIX), noise levels in payoffs ($q = 1\%$ or 5%), and dimension d of the simplices considered. In all cases, the number of nodes is 50, the number of observations is 95 and $\rho = 0.5$. Note that in two cases, there were no true positive nor false positives; this led to the denominator of the expression for the MCC to vanish, and the MCC itself being undefined. We have marked these two cases as UD.

Method	ACC/TPR/PPV/TNR/ F_1 /MCC/AUROC/AUPR													
(Net type, ψ , d)	(NPA, 1%, 1)							(NPA, 1%, 2)						
PBP	0.92/0.52/0.91/0.99/0.66/0.65/0.75/0.75							0.98/0.20/0.07/0.99/0.10/0.11/0.60/0.14						
GLO	0.85/0.04/0.41/0.99/0.07/0.09/0.52/0.30							0.99/0.04/0.02/0.99/0.03/0.02/0.52/0.03						
GLOC	0.99/0.99/0.95/0.99/0.97/0.96/0.99/0.97							0.99/0.99/0.30/0.99/0.46/0.54/0.99/0.64						
(Net type, ψ , d)	(NPA, 5%, 1)							(NPA, 5%, 2)						
PBP	0.91/0.48/0.87/0.99/0.56/0.58/0.73/0.71							0.98/0.34/0.08/0.99/0.13/0.16/0.67/0.21						
GLO	0.85/0.06/0.52/0.99/0.10/0.14/0.52/0.36							0.99/0.07/0.03/0.99/0.04/0.04/0.53/0.05						
GLOC	0.99/0.99/0.95/0.99/0.97/0.96/0.99/0.97							0.99/0.99/0.30/0.99/0.46/0.54/0.99/0.64						
(Net type, ψ , d)	(PA, 1%, 1)							(PA, 1%, 2)						
PBP	0.91/0.43/0.90/0.99/0.58/0.58/0.71/0.71							0.98/0.14/0.05/0.99/0.07/0.08/0.56/0.10						
GLO	0.85/0.04/0.45/0.99/0.07/0.09/0.51/0.31							0.99/0.01/0.01/0.99/0.01/0.00/0.50/0.01						
GLOC	0.99/0.99/0.95/0.99/0.97/0.96/0.99/0.97							0.99/0.99/0.31/0.99/0.47/0.55/0.99/0.65						
(Net type, ψ , d)	(PA, 5%, 1)							(PA, 5%, 2)						
PBP	0.87/0.23/0.80/0.99/0.35/0.38/0.61/0.57							0.99/0.04/0.02/0.99/0.02/0.02/0.51/0.03						
GLO	0.63/0.40/0.46/0.67/0.20/0.15/0.53/0.47							0.99/0.04/0.02/0.99/0.03/0.02/0.52/0.03						
GLOC	0.94/0.66/0.65/0.99/0.64/0.62/0.82/0.68							0.99/0.66/0.20/0.99/0.31/0.36/0.83/0.43						
(Net type, ψ , d)	(MIX, 1%, 1)							(MIX, 1%, 2)						
PBP	0.87/0.21/0.82/0.99/0.33/0.37/0.60/0.57							0.98/0.04/0.03/0.99/0.03/0.03/0.52/0.04						
GLO	0.89/0.34/0.50/0.99/0.35/0.35/0.67/0.47							0.99/0.34/0.14/0.99/0.18/0.21/0.67/0.24						
GLOC	0.99/0.99/0.96/0.99/0.97/0.97/0.99/0.97							0.99/0.99/0.41/0.99/0.47/0.63/0.99/0.70						
(Net type, ψ , d)	(MIX, 5%, 1)							(MIX, 5%, 2)						
PBP	0.87/0.16/0.78/0.99/0.27/0.31/0.58/0.53							0.98/0.02/0.02/0.99/0.02/0.01/0.51/0.02						
GLO	0.90/0.36/0.65/0.99/0.38/0.39/0.67/0.55							0.99/0.34/0.14/0.99/0.18/0.21/0.66/0.24						
GLOC	0.89/0.35/0.55/0.99/0.36/0.36/0.67/0.50							0.99/0.33/0.14/0.99/0.20/0.21/0.66/0.24						

Table S3. **The GLOC method performs consistently better than PBP and GLO when the measured strategy matrix is contaminated by noise.** Values of accuracy (ACC), true positive rate (TPR), positive predictive value (PPV), true negative rate (TNR), F_1 score, Matthews correlation coefficient (MCC), as well as the area under the receiver operating characteristic curve (AUROC) and that under the precision-recall curve (AUPR) for noisy data from a Prisoner’s Dilemma game show that, despite sharp drops across different metrics compared with those in contaminated payoffs, GLOC still reaches the highest ones especially when tiny noise exists in strategies. The results are reported by the type of synthetic simplicial complex model, amount of noise ψ in strategies and dimension d of the simplices considered.

Method	ACC/TPR/PPV/TNR/ F_1 /MCC/AUROC/AUPR													
(Net type, q, d)	(Malawi, 0%, 1)							(Malawi, 0%, 2)						
PBP	1.00/1.00/0.99/1.00/1.00/1.00/1.00	1.00/1.00/0.69/1.00/0.81/0.83/1.00/0.84												
GLO	1.00/1.00/0.99/1.00/0.99/0.99/1.00/0.99	1.00/1.00/0.96/1.00/0.98/0.98/1.00/0.98												
GLOC	0.99/1.00/0.91/0.99/0.95/0.95/1.00/0.95	1.00/1.00/0.92/1.00/0.96/0.96/1.00/0.96												
(Net type, q, d)	(Malawi, 1%, 1)							(Malawi, 1%, 2)						
PBP	1.00/1.00/1.00/1.00/1.00/1.00/1.00	1.00/1.00/0.77/1.00/0.87/0.88/1.00/0.88												
GLO	1.00/1.00/0.97/1.00/0.99/0.99/1.00/0.99	1.00/1.00/0.98/1.00/0.99/0.99/1.00/0.99												
GLOC	1.00/1.00/0.99/1.00/0.99/0.99/1.00/0.99	1.00/1.00/0.97/1.00/0.99/0.99/1.00/0.99												
(Net type, q, d)	(Malawi, 5%, 1)							(Malawi, 5%, 2)						
PBP	1.00/1.00/1.00/1.00/1.00/1.00/1.00	1.00/1.00/0.73/1.00/0.84/0.86/1.00/0.87												
GLO	1.00/1.00/0.95/1.00/0.97/0.97/1.00/0.98	1.00/1.00/1.00/1.00/1.00/1.00/1.00/1.00												
GLOC	1.00/1.00/0.98/1.00/0.99/0.99/1.00/0.99	1.00/1.00/0.99/1.00/1.00/1.00/1.00/1.00												
(Net type, q, d)	(SFHH, 0%, 1)							(SFHH, 0%, 2)						
PBP	1.00/1.00/1.00/1.00/1.00/1.00/1.00	1.00/1.00/0.71/1.00/0.83/0.84/1.00/0.85												
GLO	1.00/1.00/0.96/1.00/0.98/0.98/1.00/0.98	1.00/1.00/1.00/1.00/1.00/1.00/1.00/1.00												
GLOC	1.00/1.00/0.99/1.00/1.00/1.00/1.00/1.00	1.00/1.00/0.99/1.00/0.99/0.99/1.00/0.99												
(Net type, q, d)	(SFHH, 1%, 1)							(SFHH, 1%, 2)						
PBP	1.00/1.00/0.99/1.00/1.00/1.00/1.00	1.00/1.00/0.81/1.00/0.89/0.90/1.00/0.90												
GLO	1.00/1.00/0.98/1.00/0.99/0.99/1.00/0.99	1.00/1.00/0.98/1.00/0.99/0.99/1.00/0.99												
GLOC	1.00/1.00/0.99/1.00/0.99/0.99/1.00/0.99	1.00/1.00/1.00/1.00/1.00/1.00/1.00/1.00												
(Net type, q, d)	(SFHH, 5%, 1)							(SFHH, 5%, 2)						
PBP	1.00/0.98/1.00/1.00/0.99/0.99/0.99/0.99	1.00/0.99/0.73/1.00/0.84/0.85/0.99/0.86												
GLO	1.00/1.00/0.94/1.00/0.97/0.97/1.00/0.97	1.00/1.00/1.00/1.00/1.00/1.00/1.00/1.00												
GLOC	1.00/1.00/0.99/1.00/1.00/1.00/1.00/1.00	1.00/1.00/0.97/1.00/0.99/0.99/1.00/0.99												
(Net type, q, d)	(LH10, 0%, 1)							(LH10, 0%, 2)						
PBP	1.00/0.99/1.00/1.00/0.99/0.99/1.00/0.99	1.00/1.00/0.64/1.00/0.78/0.80/1.00/0.82												
GLO	0.99/1.00/0.94/0.99/0.97/0.96/1.00/0.97	1.00/1.00/0.99/1.00/0.99/0.99/1.00/0.99												
GLOC	1.00/1.00/0.99/1.00/0.99/0.99/1.00/0.99	1.00/1.00/0.98/1.00/0.99/0.99/1.00/0.99												
(Net type, q, d)	(LH10, 1%, 1)							(LH10, 1%, 2)						
PBP	1.00/0.98/1.00/1.00/0.99/0.99/0.99/0.99	1.00/0.98/0.77/1.00/0.86/0.87/0.99/0.87												
GLO	0.99/1.00/0.95/0.99/0.97/0.97/1.00/0.97	1.00/1.00/1.00/1.00/1.00/1.00/1.00/1.00												
GLOC	1.00/1.00/0.99/1.00/1.00/0.99/1.00/1.00	1.00/1.00/0.99/1.00/1.00/1.00/1.00/1.00												
(Net type, q, d)	(LH10, 5%, 1)							(LH10, 5%, 2)						
PBP	0.97/0.77/1.00/1.00/0.87/0.86/0.88/0.90	1.00/0.61/0.70/1.00/0.65/0.65/0.80/0.65												
GLO	1.00/1.00/0.99/1.00/0.99/0.99/1.00/0.99	1.00/0.73/1.00/1.00/0.75/0.77/0.87/0.87												
GLOC	1.00/1.00/0.99/1.00/1.00/1.00/1.00/1.00	1.00/1.00/0.99/1.00/1.00/1.00/1.00/1.00												

Table S4. **The GLO and GLOC methods perform better than PBP on empirical complexes when the measured payoff matrix is contaminated by noise.** Values of accuracy (ACC), true positive rate (TPR), positive predictive value (PPV), true negative rate (TNR), F_1 score, Matthews correlation coefficient (MCC), as well as the area under the receiver operating characteristic curve (AUROC) and that under the precision-recall curve (AUPR) show that all three methods perform well in the reconstruction of 1-simplices without noise. However, GLO and GLOC outperform PBP on 2-simplices. This difference is amplified when noise is added to the data, in which case GLOC is the only method that maintains a good performance. The results are reported by data set, amount of noise q and dimension d of the simplices considered.

Method	ACC/TPR/PPV/TNR/ F_1 /MCC/AUROC/AUPR									
(Net type, ψ , d)	(Malawi, 1%, 1)					(Malawi, 1%, 2)				
PBP	0.99/0.91/0.87/0.99/0.89/0.88/0.95/0.90					0.99/0.79/0.11/0.99/0.20/0.29/0.89/0.45				
GLO	0.99/0.93/0.87/0.99/0.90/0.89/0.96/0.90					0.99/0.22/0.04/0.99/0.06/0.08/0.60/0.13				
GLOC	0.99/0.96/0.88/0.99/0.92/0.91/0.97/0.92					0.99/0.99/0.15/0.99/0.25/0.38/0.99/0.57				
(Net type, ψ , d)	(Malawi, 5%, 1)					(Malawi, 5%, 2)				
PBP	0.96/0.56/0.80/0.99/0.66/0.65/0.77/0.70					0.99/0.25/0.04/0.99/0.07/0.10/0.62/0.15				
GLO	0.93/0.14/0.49/0.99/0.22/0.24/0.57/0.35					0.99/0.01/0.00/0.99/0.00/0.00/0.50/0.01				
GLOC	0.77/0.35/0.48/0.80/0.26/0.25/0.58/0.44					0.99/0.41/0.06/0.99/0.11/0.16/0.70/0.24				
(Net type, ψ , d)	(SFHH, 1%, 1)					(SFHH, 1%, 2)				
PBP	0.98/0.77/0.85/0.99/0.80/0.79/0.88/0.82					0.99/0.51/0.11/0.99/0.18/0.23/0.75/0.31				
GLO	0.94/0.24/0.44/0.99/0.26/0.28/0.61/0.36					0.99/0.06/0.01/0.99/0.02/0.02/0.52/0.04				
GLOC	0.98/0.82/0.85/0.99/0.83/0.82/0.90/0.84					0.99/0.96/0.20/0.99/0.33/0.43/0.97/0.58				
(Net type, ψ , d)	(SFHH, 5%, 1)					(SFHH, 5%, 2)				
PBP	0.95/0.41/0.75/0.99/0.53/0.53/0.70/0.60					0.99/0.07/0.02/0.99/0.03/0.03/0.53/0.04				
GLO	0.92/0.16/0.25/0.98/0.15/0.14/0.57/0.23					0.99/0.01/0.00/0.99/0.00/0.00/0.50/0.01				
GLOC	0.94/0.26/0.65/0.99/0.36/0.38/0.62/0.48					0.99/0.38/0.09/0.99/0.14/0.18/0.68/0.23				
(Net type, ψ , d)	(LH10, 1%, 1)					(LH10, 1%, 2)				
PBP	0.93/0.47/0.86/0.99/0.61/0.61/0.73/0.69					0.98/0.20/0.10/0.99/0.13/0.13/0.59/0.15				
GLO	0.89/0.04/0.34/0.99/0.07/0.08/0.52/0.24					0.98/0.01/0.01/0.99/0.01/0.00/0.50/0.01				
GLOC	0.95/0.63/0.88/0.99/0.72/0.72/0.81/0.78					0.99/0.77/0.32/0.99/0.45/0.49/0.88/0.54				
(Net type, ψ , d)	(LH10, 5%, 1)					(LH10, 5%, 2)				
PBP	0.92/0.39/0.78/0.99/0.48/0.50/0.69/0.62					0.98/0.21/0.07/0.99/0.11/0.12/0.60/0.15				
GLO	0.88/0.03/0.25/0.99/0.05/0.05/0.51/0.19					0.98/0.01/0.01/0.99/0.01/0.00/0.50/0.01				
GLOC	0.94/0.99/0.11/0.03/0.20/0.05/0.51/0.55					0.98/0.19/0.10/0.99/0.13/0.13/0.59/0.14				

Table S5. **GLOC performs the best to reconstruct empirical complexes when tiny noise exists in a strategy matrix.** Values of accuracy (ACC), true positive rate (TPR), positive predictive value (PPV), true negative rate (TNR), F_1 score, Matthews correlation coefficient (MCC), as well as the area under the receiver operating characteristic curve (AUROC) and that under the precision-recall curve (AUPR) show that GLOC consistently outperforms the other two methods to reconstruct 2-simplices when a minority part ($\psi = 1\%$) of strategies have been mistaken into the opposite ones. The results are reported by data set, amount of noise ψ in strategies and dimension d of the simplices considered.

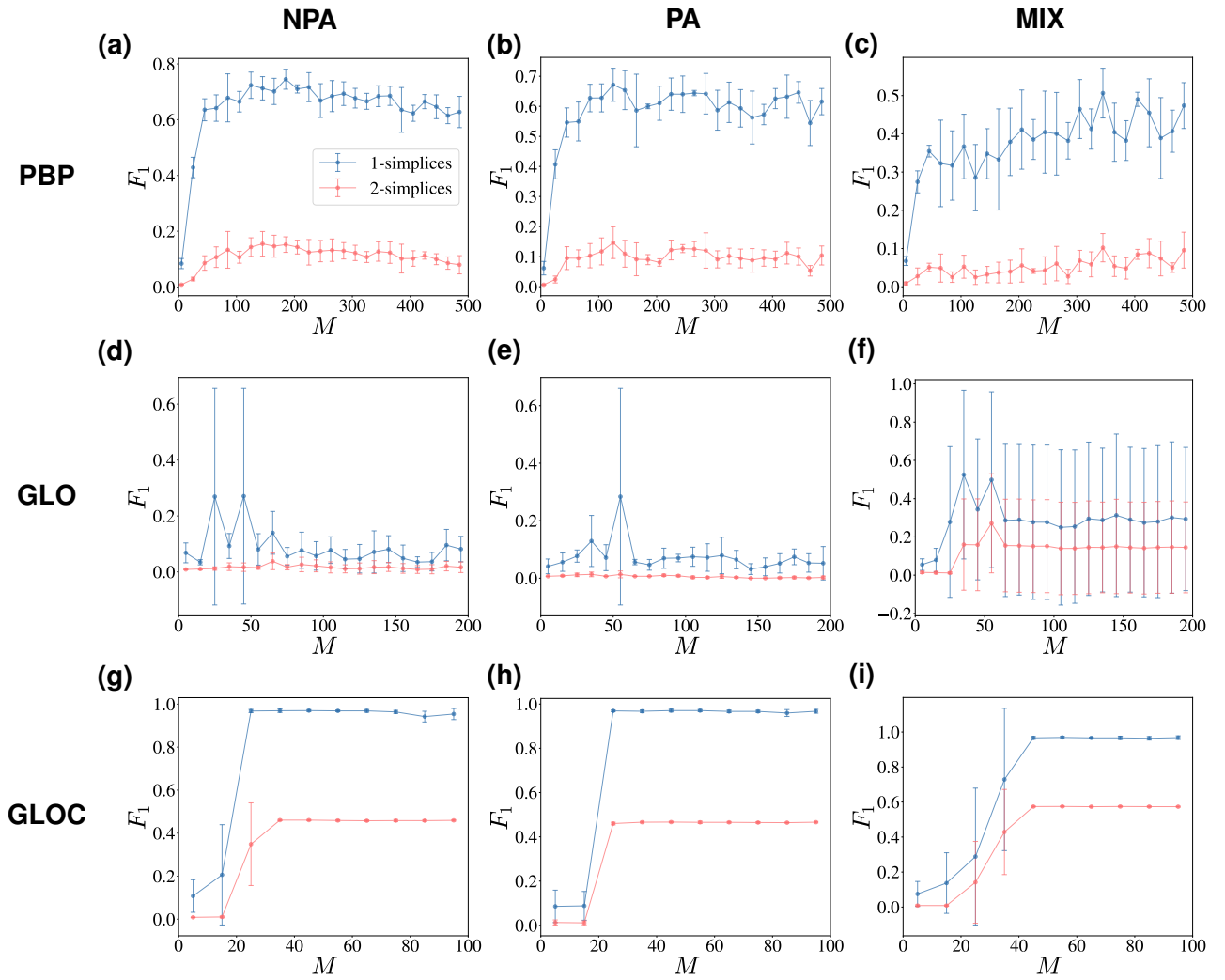


Figure S1. **GLOC outperforms PBP and GLO for noisy data in strategies.** In sharp contrast to the results of contaminated payoffs (Fig. 3), the performance of all three methods on noisy data ($\psi = 1\%$) of strategies from a Prisoner's Dilemma game drops. However, GLOC still reaches the highest F_1 scores to reconstruct both 1-simplices (blue) and 2-simplices (red) in all of three synthetic simplicial complex models. Meanwhile, GLOC requires the minimum size of the observation set M to reach $F_1 \geq 0.4$.

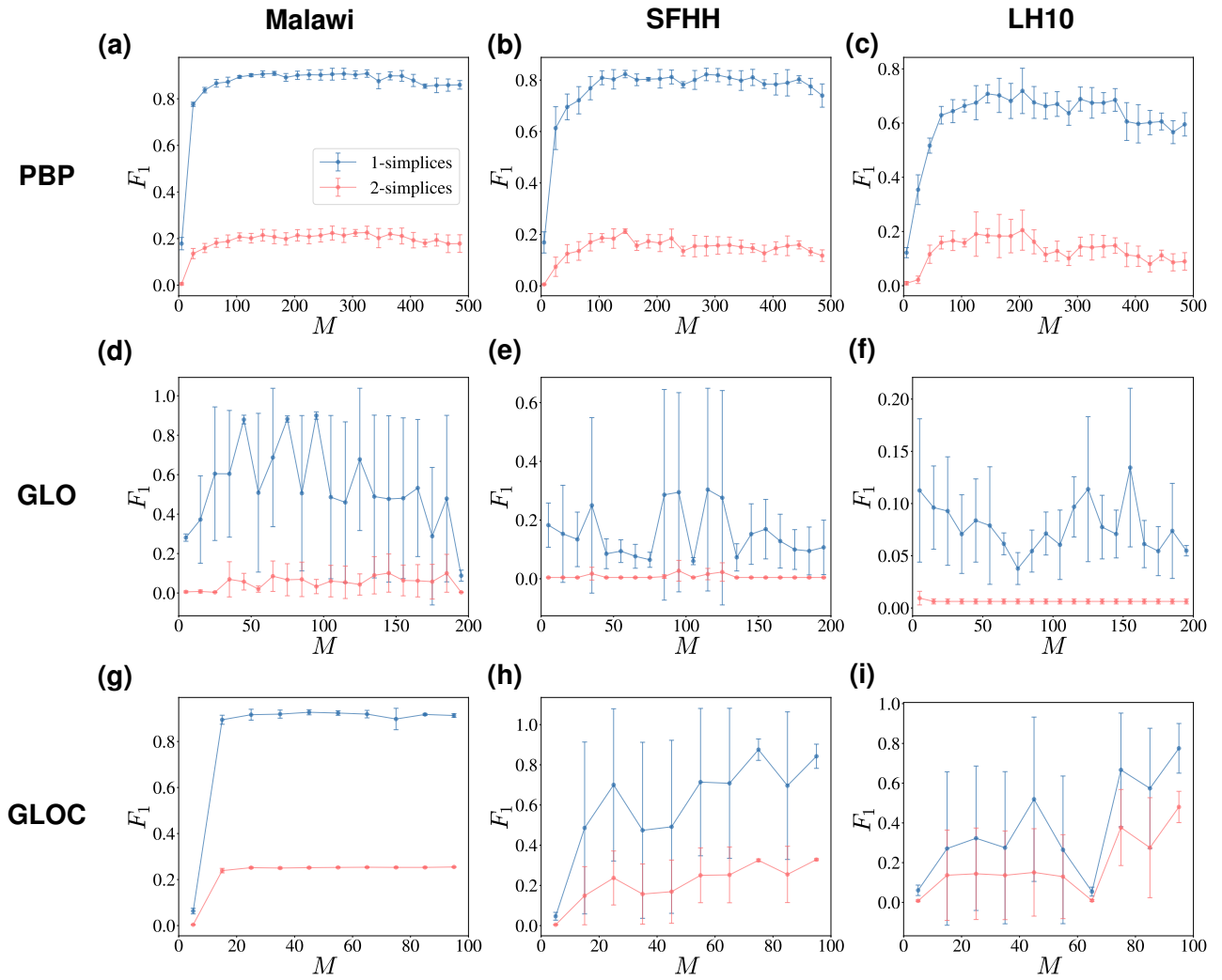


Figure S2. **GLOC is the best performing method to reconstruct empirical complexes with contaminated strategies.** The relative performance of GLO on noisy data ($\psi = 1\%$) in strategies from a Prisoner's Dilemma game drastically drops with respect to the noiseless case (Fig. 4). Meanwhile, compared with other two methods, GLOC can still obtain a relatively higher F_1 score with the smallest observation data sets.